Sub-Sahara African Academic Research Publications
June, 2021, Editions

JECM
Journal of Environmental Design and Construction Mgt.
Vol.20, No.4, ISSN 2292-7733

ANALYSIS IN EXPOSURE TO HEAT IN JIMETA RESIDENTIAL NEIGHBOURHOOD IN ADAMAWA STATE, USING SPARTIAL SYNOPTIC CLASSIFICATION SYSTEM

TANKO, BINIBONORI SALIHU
Department of Urban and Regional Planning, Federal Polytechnic Mubi, Adamawa state

Abstract:
The Urban Heat Island (UHI) is defined as elevated surface and air temperatures in urban areas relative to surrounding suburban and exurban areas (Solecki et al., 2005). Problems that result from the UHI include decreased air quality, increased heat mortality, increased energy and water use, failure of infrastructure, and altered regional precipitation patterns (Stone, 2005; Gartland, 2008; Baik et al, 2000). Adamawa state Urban Planning Development Authority is increasingly taking action to analyze and reduce UHIs. Yet, past research provides insufficient information for researchers and planners on 1) the relative contribution of neighborhood physical characteristics to UHIs and how those physical characteristics' contribution may change during different times of day, 2) the accuracy of land cover quantifications necessary to predict UHIs, This study examines how different physical features measured at the neighborhood scale contribute to the UHI intensity in eight (8) residential neighborhoods in Jimeta metropolitan area of Adamawa state using synoptic classification system. During the dry season of 2019, we collected air temperature measurements in neighborhoods selected to represent different land cover mixes, neighborhood building configurations, and adjacent heat sources and sinks. Consistent with coarse-scale investigation that rely on surface temperature proxies, the predictors with the most explanatory power of elevated air temperatures at night were land cover variables. We found that light winds at night resulted in stronger relationships between the physical characteristic variables and UHI intensity at 2 a.m.

(adjusted R2 = 0.68) than at 4 p.m. (adjusted R2 = 0.26). At night percent impervious was a better predictor of UHIs relative to building configuration. The relationships changed during the day. The significant predictor of UHI intensity shifted to upwind adjacent factors during the afternoon likely due to higher wind speeds. During the afternoon we found that a neighborhood's distance to upwind industrial areas was a better predictor of UHIs relative to land cover factors. This research is an important contribution to understanding how municipalities embarking on UHI reduction should prioritize limited financial and political resources to reduce the heat vulnerability of residents.

Keywords: *Urban Heat Islands, Urban Heat Island Evaluation, Urban Climatology, Heat Vulnerability, Urban Climate Planning*

Introduction

By changing the reflectivity and energy balance of land, the built environment alters its climate and produces distinct microclimates (Gartland, 2008; Stone, 2012). The most problematic outcome of the built environment's influence is referred to as the Urban Heat Island effect (UHI). The UHI is defined as elevated urban air and surface temperatures relative to surrounding suburban and exurban areas (Solecki *et al*., 2005). Often expressed in terms of the degrees difference relative to cooler locations, areas with elevated UHIs increase residents' vulnerability to heat related illness and death, especially in summer (Gartland, 2008; Memon *et al.* 2007; O'Neill *et al*, 2005; Harlan *et al.*, 2006). Research has found that in cities of the world the UHI increased air temperatures by 7 oC in London, United Kingdom (Wilby, 2003), 6.5 oC in Shanghi, China (Djen *et al.*, 1994), and 12 ˚C in Lodz, Poland (Klysik and Fortuniak, 1999). While the UHI is a distinct phenomenon from global climate change, increasing temperatures and changing precipitation patterns are exacerbating its negative impacts (Stone, 2012). While UHIs can have some positive outcomes in wintertime (Oke, 1988; Santamouris *et al*., 2007), UHIs are largely problematic in warm weather. Fortunately, our knowledge of UHI patterns has advanced over the last forty years. We now understand that urban areas may contain many dispersed UHIs that change diurnally and are not limited to the urban core. In addition, UHI patterns depend on regional atmospheric transport, maritime

influences, and land cover dynamics (Jenerette *et al*., 2007; Gaffin *et al*, 2008, Gray and Finster, 2000).
Ensuring safe, livable conditions in cities requires understanding where UHIs exist and how we can lessen their negative impacts during dry season months. The cities of Albuquerque, Boise, Chicago, Hartford, Louisville, Minneapolis, New York, Philadelphia, Pittsburgh, and Portland currently have started UHI reduction programs (Stone, 2012). These programs generally seek to change the physical characteristics of neighborhoods based on UHI identification using measures of regional land cover derived from satellite images of surface temperatures. Improving our understanding of how the characteristics of land cover, neighborhood building configuration, and adjacent heat sources and sinks differentially contribute to urban climatology and meteorology will help urban planners determine the information they must collect to understand neighborhood microclimate variation so they can prioritize strategies to lessen the UHI negative effects. Although past research has looked at these physical characteristics separately, these three types have not been examined in combination. The value of this study is the examination of multiple potential factors to determine the ones that researchers and planners should prioritize.

Research Questions

This study examines how the physical characteristics of eight neighborhoods in Jimeta differentially contribute to elevated air temperatures. Specifically. we investigate three research questions. First, how do the physical characteristics of land cover, neighborhood configuration, and adjacent heat sources and sinks contribute to elevated summer air temperatures in eight residential neighborhoods? Second, does the relative contribution of the factors vary in importance between nighttime and daytime? Finally, the third research question investigates whether the factors that explain nighttime and daytime UHIs shift in importance during a heat event. Based on the urban microclimate literature, we expect that fine-grained measures of percent impervious and the percent tree canopy will be the most important influence on microclimate temperatures for both night and daytime. However, based on the diurnal variation in wind speed, we hypothesize that neighborhood building configuration variables of urban canyon and orientation will be important in explaining nighttime temperatures while adjacent heat sources and sinks will be more important during the daytime when wind speeds are greater.

Materials and Methods

Study neighborhoods

We used a simple random sampling to select eight (8) residential wards of Yola North Local Government Area. These selected residential neighborhoods comprises of high, middle, and lower income neighborhoods variation. The selected neighborhoods were Luggere, Nasarawo, Alkalawa, Doubeli, Karewa, Limawa, Yelwa and Ajiya residential neighbourhoods. Within each of the selected neighborhoods, we selected one representative city block in which to take air temperature, relative humidity, and to calculate the physical characteristics. The study was conducted with four east-west oriented alleys Ajiya ward, Yelwa ward, Limawa ward and Luggere ward) and four neighborhoods with north-south oriented alleys (Alkalawa ward, Doubeli ward, Karewa ward and Nassarawo wards) to understand how orientation may influence canyon shading and ventilation and thus contribute to air temperatures.

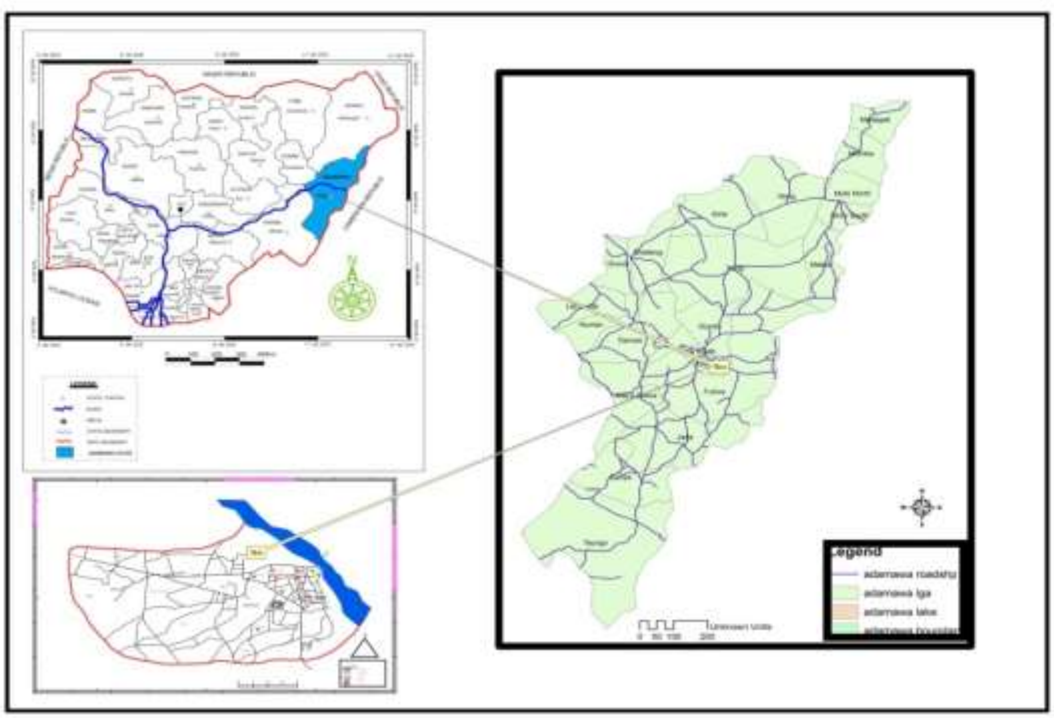

Figure 1.1 Locational Map showing the study Area

Figure 1.2 Map illustrating the city of Jimeta limits, the eight study neighborhood, Yola International Airport.

Social Characteristics in 2019

Table 1.1 below describes each neighborhood's social and physical characteristics. Average household income in 2019 was lowest in the neighborhoods of Doubeli ward which is N30, 000 per month while the highest Alkalawa and Karewa wards had the highest monthly per capital income of N46, 000 and N44, 000 respectively., In 2019, population density varied from a low of 30.0 people per hectare (12.1 people per acre) in Ajiya ward to a high of 94.8 people per hectare (38.4 people per acre) in Luggere ward.

Table 1.1: Descriptive Statistics of Neighborhood Social, Density, and Land Cover Characteristics for Jimeta Residential Neighborhoods in 2019

	SOCIAL CHARACTERISTIC	DENSITY		LAND COVERS		
Neighbourhood	**Average Household Monthly Income**	**Density Unit M2**	**Density People %**	**% Impervious Surfaces**	**% Roof Covers**	**% Tree Canopy**
Luggere Ward	33,000	47.4	94.8	95.7	34	4.7
Ajiya Ward	35,000	14.3	30.0	54.6	22.9	60.4
Nasarawo Ward	41,000	27.0	70.6	88.1	37.9	13.2
Limawa Ward	31,000	30.9	55.1	94.3	39.1	29.4

Karewa Ward	44,000	26.0	83.5	78	37.9	18.1
Alkalawa Ward	46,000	19.2	56.8	73.5	31.9	23.1
Yelwa Ward	39,000	35.3	92.0	75.1	28.2	19.7
Doubeli Ward	30,000	35.7	58.9	79.9	21.8	18.5

* Social Characteristics and Densities are from fieldwork 2019.

** Calculated by authors.2019

Table 1.2: Descriptive Statistics of Building Configuration and Adjacent Heat Sources and Sinks for Eight Jimeta Neighborhoods in 2019

	Neighborhood Building Configuration**				Adjacent Heat Sources and Sinks**						
Neighborhood	Urban Canyon Ratio	Average Build Heights on Block (m)	Sky View Factor	Orientation	% Tree Canopy Upwind Area	Average Build Heights in Upwind Area (m)	Distance to River (km)	Distance to Down-town (km)	Distance to Industrial (km)	Distance to Freeway (km)	Distance to Park (km)
Luggere Ward	0.78	13.8	0.53	E-W	11.0	14.3	3.6	3.3	2.6	4.8	4.4
Ajiya Ward	0.24	9.1	0.51	E-W	49.5	9.1	11.5	19.2	5.9	7.5	2.7
Nasarawo Ward	0.44	12.4	0.66	N-S	8.3	12.2	8.0	8.3	0.2	8.1	11.5
Limawa Ward	0.6	13	0.49	E-W	30.0	15.2	3.7	2.1	1.7	7.3	9.2
Karewa Ward	0.32	10.4	0.67	N-S	12.7	10.4	11.6	12.4	1.4	9	1
Alkalawa Ward	0.29	9.9	0.69	N-S	18.1	9.8	0.4	20.3	1.9	7.1	1.5
Yelwa Ward	0.31	10.8	0.7	E-W	23.3	10.7	11.4	10.5	2.1	4.5	6.5
Doubeli Ward	0.28	9.1	0.65	N-S	14.0	10.7	1.4	4.6	1.6	1.1	9.1

**Calculated by author, 2019
Orientation (north-south or east-west)
Distance from each to River Benue is a straight line (not in upwind direction)
Distance from each block to downtown is a straight (not in upwind direction)
Distance from each block to upwind (southwest) industrial areas, highway, and park is a straight line.

Neighborhood physical characteristics

The eight neighborhoods varied in compactness with the density of units per hectare in 2019 ranging from a low of 14.3 units per hectare (5.8 units per acre) in Ajiya ward to a high of 47.4 units per hectare (19.2 units per acre) in Luggere ward. Ajiya ward had the lowest amount of impervious surface with 54.6 %, while Luggere ward had the highest with 95.7%. Similarly Ajiya ward had the highest tree canopy with 60.4% coverage and Luggere ward the lowest with 4.7% coverage. Yet, the amount of tree canopy was not an inverse relationship with the amount of impervious surface area. Luggere ward and Limawa ward both had roughly 95% impervious surface areas, but while Luggere ward had less than 5% tree canopy Limawa ward had nearly 30% tree canopy. The urban canyon ratio was lowest in Ajiya ward with a h/w ratio of 0.24 and greatest in Luggere ward with a h/w ratio of 0.78. The neighborhoods' distance from River Benue ranged from 0.43 km for Alkalawa ward to more than 11 km for Karewa ward.

Weather observation instruments

We took weather observations using stationary Onset U23-002 HOBO External Temperature/RH Data Logger with sensor and a model RS3 solar radiation shield. The HOBO weather stations have an air temperature accuracy of ±0.2ºC from 0 to 50ºC and relative humidity accuracy of ±2.5% from 10 to 90% relative humidity (Onset, 2019). Additional hourly weather observations from March to April 31, 2019 were obtained from Yola International Airport located in the city of Adamawa state (figure 3.2). Data from this location is used to calculate baseline air temperature, relative humidity, wind speed and direction, and sky condition. For this study we used Yola International Airport because the predominate wind direction was out of the southwest direction (210 degrees) during the study period, so Yola International Airport (due to its more southwesterly location) provides a better comparison before air masses move over the urban neighborhoods. Although Yola International Airport is well with the Jimeta -Yola urbanized region, the airport's open character allows for ventilation and mixing of the air. In addition, the weather station is located at the center of the tarmac (see figure 3.5) west of the terminal and away from idling jets. Finally, although impervious surfaces cover roughly 61% of the airport grounds, as calculated from the manipulations of GIS on satellites imageries, the runways are lighter colored concrete that would absorb less solar radiation than asphalt.

Data collection procedures:

In locating the HOBO units, we used the *Initial Guidance to Obtain Representative Meteorological Observations at Urban Sites* criteria (Oke, 2004) to establish the locations and heights of the equipment. Each HOBO unit was mounted on the north or east side of a utility pole at a height of three meters (above the height of truck traffic) at the center of each neighborhood block's pathway collecting ambient air temperature and relative humidity every 5 minutes for 24 hours a day from March 1 to April 31, 2019. The placement was within the urban canopy layer as residential building heights were at minimum 9.14 meters. The solar radiation shield was mounted to the utility pole with two screws and two zip ties to secure the station and the data logger with the logger window facing upwards. Data were downloaded every two weeks using a HOBO data shuttle to transfer the data from each weather station to a laptop computer. We chose two important times during the day to focus on for the analysis. I used the time of 2 a.m. in the analysis because past research (Kalkstein and Davis, 1989) has pointed to the importance of cooling relief at night for human well-being. We also selected 4 p.m. because it was the statistical average time for maximum daily highs over the two-month period. The UHI intensity or the difference in air temperature (ΔTair) between the eight neighborhoods and Yola International Airport was calculated for both 2 a.m. and 4 p.m. ΔTair at 2 a.m. and 4 p.m. serves as the dependent variable in the analysis.

Quantifying neighborhood physical characteristics

We quantified 15 independent variables for the study including density, land cover, neighborhood building configuration, and adjacent heat sources and sink variables (Tables 3.1 and 3.2). Density of units per acre was calculated using GIS, calculating all land cover percentages including impervious surfaces, roof cover, and tree canopy. Using a similar method to Akbari and colleagues (2003), three-dimensional impervious surface was calculated by hand in AutoCAD (an architectural drafting program) as the percentage of the whole block including a portion of the street's impervious surface extended out from street curb to mid street. The urban canyon ratio was calculated as the average height of the block's buildings to the width of the alley and backyard space at each collection location.

Neighborhood building configuration variables were building heights, urban canyon ratio, SVF, and urban canyon orientation. Average building heights was calculated using measuring take and professional judgment while urban canyon ratio for each block were calculated as height of the building vs. Wight of the street, site visits, and the Greater Yola Master Plan/ Zonning code Summary of standard building heights for each neighborhoods building type. Sky view factors (SVF) were calculated at ground level below each weather station similar to Svensson (2004) using a Solmetric SunEye. Orientation of the urban canyon was calculated as a dummy variable, either 0 for north-south oriented alleys or 1 for east-west oriented alleys.

The UHI intensity or the difference in temperature between each neighborhood and Yola International Airport was calculated for 2 a.m. and 4 p.m. for 12 clear days in March and April, 2019. For the ellipse of adjacent heat sources and sinks we calculated both percentage of tree canopy (heat sink) and average building heights (heat source) for a 0.5 km long elliptical source area to the southwest (upwind) of each HOBO weather station. Finally, we quantified the distances from the neighborhood to River Benue, downtown Jimeta, and other potential heat sources and sinks to the southwest (upwind) of each neighborhood.

Results

Although not an extremely dry season in terms of the number of heat events, the dry season of 2019 was consistently warm. To begin, we explored the effect of controlling for heat event days, clear skies, and heat event days with clear skies to understand how this affected UHI intensity (ΔTair). Table 3.3 describes four different types of UHI intensity or ΔTair analysis between the neighborhoods and Yola International Airport during March and April 2019 using data from 1) all 62 days, 2) 12 heat event days with or without cloud cover only, 3) 12 clear days only, and 4) two clear heat event days only. First, to select the 12 heat event days (clear and cloudy) we used Sheridan’s (2012) Spatial Synoptic Classification System to identify days when the combination of heat and humidity pose a dangerous threat to residents. Then, to isolate urban factors that contributed to the warming (UHI) in the eight neighborhoods, we selected only days with clear skies with light winds (24 hours of clear skies and relatively light winds) as recommended by urban climate researchers (Stewart, 2011;

Bonacquisti *et al.,* 2006; Gedzelman *et al*., 2003; Kim and Baik, 2002; Klysik and Fortuniak, 1999; McPherson *et al*., 1997). This reduced the number of days analyzed from 62 days to 12 clear days. Finally, of the 12 clear days we selected the only two clear days, to again isolate the urban-induced warming.

Generally controlling for clear skies raises the average UHI intensity for all neighborhoods by +0.11ºC at 2 a.m. and +0.42ºC from all 62 days. Although this is not much, at 2 a.m. the range in UHI intensities (ΔTair) increases from 2.97ºC during all 62 days to 4.15ºC during the 12 clear days. At night, controlling for weather (clear skies) resulted in Ajiya ward with more intense cool island conditions (lower air temperature than Yola International Airport) and Luggere ward with more intense UHI conditions. During the day the change in the range of UHI intensities is not as large (from 2.28ºC for all 62 days to 2.85ºC for the 12 clear days). This finding suggests the benefits of controlling for weather to isolate urban-induced warming from other warming effects.

As for the neighborhoods compared to Yola International Airport (ΔTair), for the 12 clear days, the warmest neighborhood at night was Luggere ward averaging +2.34º C ±0.73 warmer than Yola International Airport. The coolest neighborhood was Ajiya ward, with average air temperatures -1.81ºC ± 0.85 cooler than Yola International Airport. During the day the ordering of the warmest to coolest neighborhoods shifted. Karewa ward unseated Luggere ward as the warmest neighborhood during the late afternoon (with average readings +2.68ºC ±0.59 warmer than Yola International Airport). At 4 p.m. in the afternoon, Ajiya ward still ranked as the coolest neighborhood. The accuracy of the HOBO weather stations was ±0.20ºC. Finally, through ANOVA analysis we found that there was a statistically significant difference between neighborhoods air temperature at both 2 a.m. ($F = 28.91$, $df = 7, 88$) and 4 p.m. ($F = 6.04$, $df = 7, 88$) at the 0.001 level.

Our results show that the warmest neighborhoods during the 12 clear days (Luggerre ward at 2 a.m. and Karewa ward at 4 p.m.) were not the poorest neighborhoods. In this small sample of eight neighborhoods there was no correlation between elevated air temperature and average household income contrary to previous studies that link low amounts of vegetation and low income to hotter neighborhoods (Jenerette *et al.,* 2007; Santamouris *et al.,* 2007; Harlan *et al.,* 2006; Solecki *et al.,* 2005). The lowest income neighborhood (Doubeli ward with an average household income in 2019 of N30,000 had 18.5% tree canopy. Whereas higher income neighborhoods such as Luggere ward and Nasarawo ward with an average household incomes in 2019 of N33,000 and N41,000 respectively had lower percentages of tree canopy (Luggerre ward 4.7% and Nasarawo 13.2% tree canopy). In addition, both Luggere ward and Nasarawo ward were consistently warmer than Doubeli ward at 2 a.m, and 4 p.m.

Table 1.3: Air Temperature from Yola International Airport during March and April, 2019

S/N	2 a.m	ALL DAYS TEMPERATURE DIFFERENCE (n= 62)	HEAT EVENT DAYS (n=12)	CLEAR DAYS (n =12)	CLEAR DAYS, HEAT EVENTS (n=2)
	NEIGHBOURHOODS				
1	**Ajiya Ward**	-1.04	-0.86	-1.81	-1.86
2	**Alkalawa Ward**	0.35	-0.06	0.41	0.39
3	**Karewa ward**	0.75	0.91	0.74	1.53
4	**Yelwa Ward**	0.83	0.93	0.84	1.38
5	**Doubeli Ward**	0.99	0.56	1.41	1.52
6	**Nasarawo Ward**	1.41	1.28	1.73	1.97
7	**Limawa ward**	1.67	1.29	2.06	2.18
8	**Luggere Ward**	1.93	1.59	2.34	2.52
	TOTAL	0.86	0.71	0.97	1.2

S/N	4 a.m	ALL DAYS TEMPERATURE DIFFERENCE (n= 62)	HEAT EVENT DAYS (n=12)	CLEAR DAYS (n =12)	CLEAR DAYS, HEAT EVENTS (n=2)
	NEIGHBOURHOODS				
1	**Ajiya Ward**	-0.06	-0.68	-0.17	-0.95
2	**Doubeli Ward**	0.9	1.12	1.76	1.4
3	**Alkalawa Ward**	0.94	1.28	1.76	0.85
4	**Luggere Ward**	1	1.27	1.33	1.1
5	**Limawa Ward**	1.01	1.27	1.57	1.75
6	**Yelwa Ward**	1.59	1.51	1.82	2.15
7	**Nasarawo ward**	2	1.93	2.23	2.3
8	**Karewa Ward**	2.22	2.27	2.68	3.3

9	TOTAL	1.2	1.24	1.62	1.49

In the first analysis, we conducted a Bivariate analysis to understand the relationship between each independent variable and the 2 a.m. and 4 p.m. ΔTair neighborhood air temperatures difference controlling for weather (12 clear days) (table 3.4). At 2 a.m. during the 12 clear days the 11 significant Bivariate correlations (p=.01) were 1) percent impervious surface (.82), 2) percent tree canopy (-.72), 3) distance to downtown (-.70), 4) upwind building heights (.67), 5) upwind industrial (-.65), 6) building heights (.63), 7) upwind tree area (-.62), 8) urban canyon ratio (.60), 9) percent of roof (.47), 10) upwind vegetation (.46), and 11) distance to River Benue (-.40). At 4 p.m. during the 12 clear days the seven significant Bivariate correlations (p=.01) were 1) upwind industrial (-.52), 2) upwind trees (-.48), 3) percent tree canopy (-.44), 4) SVF (.38), 5) orientation (-.36), 6) percent roof area (.33), and 7) percent impervious (.30). In general, both the number of independent variables and strength of the bivariate relationships between the independent variables and ΔTair were greater at 2 a.m. than at 4 pm.

Table 1.4: Bivariate Correlations between Physical Characteristics and the UHI intensity at 2 a.m. and 4 p.m. for eight Jimeta neighborhoods during 12 clear days in dry season of 2019

	UHI Intensity		UHI Intensity			Neighborhood Configuration				Adjacent Heat Sources and Sinks						
	2 am	4pm	% ISA+	% Roof	% Tree Canopy	UC++ ratio	Build Ht. of Block	SVF	Orientation (0, 1)	% Tree Canopy in Source Area	Build Ht. of Source Area	Dist. to Lake	Dist. To down-town	Dist. To Indust	Dist. To Fwys.	Dist. To Parks
Neighborhood	-.23*	-.10	-.19	.20*	.08	.01	.11	.07	-.18	-.03	-.21*	.09	.55**	11	.55**	-.22*
UHI Intensity 2 am		.19	82**	47**	-.72**	.60**	.63**	.03	-.07	-.62**	.67**	-.40**	-.70**	-.65**	-.22*	46**

UHI Intensity 4 pm			30**	33**	-.44**	.03	.12	.38**	-.36**	-.48**	.08	-.04	-.17	-.52**	.04	.10
% Impervious				67**	-.78**	.83**	.85**	-.14	.00	-.66**	.89**	-.45**	-.84**	-.70**	-.12	.51**
% Roof					-.46**	.55**	.72**	-.05	-.10	-.43**	.60**	.01	-.30**	-.59**	64**	.10
%Tree Canopy						-.49**	-.53**	-.43**	33**	.95**	-.44**	.35**	.55**	.81**	.27**	-.26*
Urban Canyon							.94**	-.55**	42**	-.30**	.92**	-.31**	-.70**	-.21*	-.00	.24*
Building Ht. of Block								-.39**	.37**	-.36**	.91**	-.15	-.66**	-.38**	.17	.37**
SVF									-.68**	-.55**	-.54**	.07	.30**	-.54**	-.12	-.05
Orientation										.60**	.39**	.25*	-.20*	.57**	-.06	-.01
% Tree Canopy Source Area											-.25*	34**	.41**	86**	.19	-.23*
Build Ht. of Source Area												-.34**	-.83**	-.36**	-.02	.49**
Distance to River Benue													.28**	.30**	44**	-.19
Distance to Downtown														47**	42**	-.67**
Distance to Industrial															04	-.49**
Distance to Freeway																-.32**

To understand the relative cumulative importance of independent factors in determining the difference in air temperature between the neighborhoods and

Yola International Airport (ΔTair), Ordinary Least Squares (O.L.S.) regression was used to regress five predictor variables in three UHI models against the dependent variable ΔTair for both 2 a.m. and 4 p.m. The independent variables that had the most significant bivariate relationships with ΔTair were used in the 2 a.m. and 4 p.m. UHI models. At 2 a.m. the bivariate correlation analysis suggested that the independent variables of land cover and building configuration factors may be the most important predictors of ΔTair. Based on the bivariate relationships, we had the following O.L.S regression UHI Models at 2 a.m.: Model 1) neighborhood location, Model 2) land cover variables for percent impervious surfaces and percent tree canopy, and Model 3) neighborhood configuration variables for the urban canyon ratio and a dummy variable representing either north-south or east-west orientation (O).

$\Delta Tair = b0 + b1N1 + b2N2 + b3N3 + b4N4 + b5N5 + b6N6 + b7N7 + b8I1 + b9C1 + b10U1 + b11O1 + e$

Dependent variable:

ΔTair = Air temperature difference (Neighborhood air temperature - Midway air temperature)

Independent variables:

N = Seven categorical dummy variable to represent the eight neighborhoods

I = Percent impervious surface

C = Percent tree canopy

U = Urban canyon ratio

O = Orientation

At 4 p.m. the bivariate analysis indicated the continued importance of land cover variables, but also the potential impact of adjacent heat sources and sinks. In the afternoon model, we substituted adjacent heat sources and sink variables for building configuration variables. Based on the bivariate relationships, we had the following O.L.S regression UHI Models at 4 p.m.: Model 1) neighborhood location, Model 2) land cover variables for percent impervious surface and percent tree canopy, and Model 3) distance to upwind industrial location and percent tree canopy in the adjacent upwind area.

$\Delta Tair = b0 + b1N1 + b2N2 + b3N3 + b4N4 + b5N5 + b6N6 + b7N7 + b8I1 + b9C1 + b10D1 + b11\ Cup\ 1 + e$

Dependent variable:
ΔTair = Air Temperature Difference (Neighborhood air temperature - Midway air temperature)
Independent variables:
N = Seven categorical dummy variable to represent the eight neighborhoods
I = Percent impervious surface
C = Percent tree canopy
D = Distance to industry
Cup = Percent upwind tree canopy

To begin the regression analysis, we wanted to understand how controlling for weather affected the explanatory power of each O.L.S regression model. We ran the 2 a.m. and 4 p.m. model using the data from 1) all 62 days, 2) 12 heat events days (clear and cloudy) only, 3) 12 clear days only, and 4) two clear heat event days only. Table 3.5 and 3.6 summarize the results of controlling for different weather conditions at 2 a.m. and 4 p.m. Controlling for weather (clear skies), when urban surfaces are more likely to affect air temperatures, improved the explanatory power of Model Three at both 2 a.m. and 4 p.m. At 2 a.m. the adjusted R2 of Model Three increased from 0.50 using the data from all 62 days to 0.68 using only the data from the 12 clear days. At 4 p.m. the adjusted R2 of Model Three increased from 0.17 using the data from all 62 days to 0.26 using only the data from the 12 clear days. This analysis confirmed that controlling for weather is a useful practice that improves the explanatory power of UHI regression models. The remainder of the results reported here are from the data with clear skies only (12 clear days and two clear heat event days).

Table 1.5 OLS Regression Analysis Comparison for UHI Intensity at 2a.m.
Methods to Calculate UHI Intensities in 2019

	Yola International Airport Clear and Cloudy Days						Yola International Airport Clear Days Only					
	All Days (n=62)			12 Heat Event Days* (n=96)			12 Clear Days* UHI (n=96)			2 Clear Days* Heat Events** UHI (n=16)		
	Model 3			*Model 3*			*Model 3*			*Model 3*		
Variable							B	SE	*Beta*	B	SE	*Beta*
Neighborhood	-0.01	0.02	-0,01	0.01	0.03	0,04	-0.02	0.04	-0.04	-0.04	0.06	-0.08

% Impervious	6.74***	1.18	0.68	5.94***	1.91	0.78	9.66***	2.58	0.82	9.27*	3.34	0.86
% Tree Canopy	-1.38***	0.48	-0.18	-1.90*	0.77	-0.31	-1.79	1.04	-0.19	-3.29*	1.35	-0.38
Urban Canyon	-1.04	0.80	-0.15	-1.75	1.29	-0.33	-1.58	1.74	-0.19	-2.3	2.26	-0.31
Orientation	0.26	0.16	0.11	0.53*	0.26	0.28	0.18	0.35	0.06	0.35	0.45	0.13
(Constant)	-3.89***	0.84		-3.22*	1.36		-5.67***	1.84		-4.46	2.39	
N		496			96			96			16	
Adjusted R2			0.50			0.58			0.68			0.90
Change in R2			0.00			0.02			0.00			0.00

*p<.05,**p<.005(one-tailed test)

Table 1.6 O.L.S Regression Analysis Comparison for UHI Intensity at 4p.m. in Eight Residential Neighbourhoods in Jimeta Using Four Different Methods to Calculate UHI Intensity in the dry season of 2019.

	Yola International Airport Clear and Cloudy Days		Yola International Airport Clear Days Only	
	All Days (n=62)	12 Heat Event Days* (n=96)	12 Clear Days* UHI (n=96)	2 Clear Days* Heat Events** UHI (n=16)
	Model 3	*Model 3*	*Model 3*	*Model 3*

Variable	B	SE	*Beta*	B	SE	*Beta*	B	SE	*Beta*	B	SE	*Beta*
Neighborhood	-0.02	0.02	-0,03	-0.004	0.06	0,01	-0.04	0.05	-0.07	-0.09	0.16	-0.15
% Impervious	-2.41**	0.90	-0.22	-1.54	2.46	-0.12	-2.2	1.97	-0.2	-2.66	6.31	-0.21
% Tree Canopy	-2.86	1.71	-0.33	-3.09	4.70	-0.29	-0.86	3.75	-0.1	-3.29	12	-0.32
Distance to Industry	-0.68***	0.13	-0.48	-0.69	0.36	-0.41	-.45*	0.18	-0.51	-0.68	0.58	-0.66
Upwind % Tree Canopy	0.02	0.02	0.21	0.02	0.06	0.12	-0.01	0.05	-0.08	0.03	0.15	0.21
(Constant)	4.16***	0.83		3.82	2.29		4.92**	1.83		5.76	5.87	
N		496			96			96			16	
Adjusted R2			0.17***			0.18			26***			0.12
Change in R2			0.06			0.05			0.09			0.12

*p < .05.**p < .01. ***p <.005 (one-tailed tests)

Examining the regression analysis using the 12 clear days only, at 2 a.m. with 96 cases, Model Three explains 68% of the variance in the ΔTair between the neighborhoods and Yola International Airport (table 3.7). Overall this model is significant with an F-value of 40.62. The only significant factor in Model Three at 2 a.m. was percent impervious of the block ($p < 0.001$ level). All other variables were not significant predictors of the ΔTair between the neighborhoods and Yola International Airport at 2 a.m. Controlling for all other factors, for every 10% increase in impervious surfaces of the block we would expect a warming of the neighborhood relative to Yola International Airport by +0.97ºC at 2 a.m. This finding confirms other studies showing the contribution of impervious surfaces to warm local temperatures. In addition, in comparison to other land cover factors neighborhood building configuration variables were not significant at 2 a.m. Interestingly, without considering building configuration Model Two had two significant factors, percent impervious ($p <$ 0.001 level) and percent tree canopy ($p < 0.05$ level). Without controlling for neighborhood building configuration, tree canopy is a significant predictor of ΔTair.

Table 1.7: Regression Analysis for UHI Temperatures at 2 a.m. in Eight Jimeta Residential Neighborhoods during 12 Clear Days in the dry season 2019

	Model 1			*Model 2*			*Model 3*		
Variable	B	SE	*Beta*	B	SE	*Beta*	B	SE	*Beta*
Neighborhood	-.12*	.05	-.23	-.05	.03	-.09	-.02	.04	-.04
% Impervious				7.42***	1.12	.63	9.66***	2.58	.82
% Tree Canopy				-2.07*	.88	-.22	-1.79	1.04	-.19
Urban Canyon							-1.58	1.74	-.19
Orientation							.18	.35	.06

(Constant)	1.58***	.31		-4.23***	1.11		-5.67***	1.84	
n		96			96			96	
Adjusted R2			.04			.68***			.68
Change in R2						.64			.00

*p < .05. **p < .01. ***p < .005 (one-tailed tests).

At 4 p.m. during the 12 clear days with 96 cases, Model Three explains 26% of the variance in the ΔTair and has one significant predictor (table 3.8). Model Three explanatory power is significantly improves over Model Two for 4 p.m. Overall, Model Three is significant with an F-value of 7.50. In this model, for every additional 1.0 km increase in distance from industrial areas we would expect a neighborhood to be -0.45ºC cooler ($p < 0.05$ level). The analysis suggests that predicting daytime ΔTair is more difficult than predicting nighttime ΔTair. In addition, higher wind speeds during the day likely displace temperatures from upwind locations, such as industrial sites.

Table 1.8: Regression Analysis for UHI Temperatures at 4 p.m. in Eight Jimeta Residential Neighborhoods during 12 Clear Days in the dry season 2019

	Model 1			*Model 2*			*Model 3*		
Variable	B	SE	*Beta*	B	SE	*Beta*	B	SE	*Beta*
Neighborhood	-.05	.05	-.10	-.04	.05	-.08	-.04	0.05	-.07
% Impervious				-1.38	1.68	-.13	-2.20	1.97	-.20
% Tree Canopy				-4.65***	1.32	-.53	-.86	3.75	-.10
Distance to Industry							-.45*	.18	-.51
Upwind % Tree Canopy							-.01	.05	-.08

(Constant)	1.86***	.29		4.00*	1.66		4.92**	1.83	
n		96			96			96	
Adjusted R2			-.00			17***			.26***
Change in R2						.19			.09

*p< .05. **p < .01. ***p < .005 (one –tailed tests).

We re-ran these models using Sheridan's (2012) Spatial Synoptic Classification (SSC) system for heat events. We had two clear days that were classified as potentially dangerous according to the SSC system. Rerunning the regression model at 2 a.m. with 16 cases, Model Three improved in explanatory power. It explained 90% of the variance in elevated air temperature (table 3.9). Overall the Model Three is significant with an F- value of 27.18. The significant factors during heat wave days were the percentage of impervious surface ($p < 0.005$ level) and percent tree canopy ($p < .01$ level). During heat event days and controlling for all other variables, for every 10% increase in impervious surfaces of the block we would expect a warming of +0.93ºC. Controlling for all other variables during heat event days, for every 10% increase in tree canopy of the block we would expect a cooling of the neighborhood relative to Midway by -0.33ºC.

$$\Delta Tair = -4.46 - 0.04N1 + 9.27I1 - 3.29C1 - 2.30U1 + 0.35O1 + e \text{ (Model Three)}$$

Table 1.9: Regression Analysis for UHI Temperatures at 2 a.m. during Heat Events in Eight Jimeta Residential Neighborhoods during Two Clear Days in the dry season of 2019

	Model 1			*Model 2*			*Model 3*		
Variable	B	SE	*Beta*	B	SE	*Beta*	B	SE	*Beta*
Neighborhood	-.15	.12	-.31	-.08	.04	-.16	-.04	.06	-.08
% Impervious				6.21***	1.40	.58	9.27*	3.34	.86
% Tree Canopy				-3.47**	1.10	-.40	- 3.29*	1.35	-.38
Urban Canyon							-2.30	2.26	-.31
Orientation							.35	.45	.13

(Constant)	1.95*	.71		-2.55	1.39		-4.46	2.39	
n		16			16			16	
Adjusted R2			.03			.91***			.90
Change in R2						.83			.00

*p < .05. **p < .01. ***p < .005 (one-tailed tests).

Running the regression model for two clear heat event days at the 4 p.m. with 16 cases, model three explained only 12% of the variance in elevated air temperature (Table 3.10). Overall the model is not significant with an F-value of 1.39. At 2 a.m., during clear heat event days the analysis suggests that the relative importance of land cover variables is higher than during the 12 clear UHI days. Both impervious surface and tree canopy become significant predictors of air temperature at 2 a.m. Yet, all predictors of air temperature are insignificant during heat events in the late afternoon (4 p.m.). This illustrates the lower ability to explain the variance in afternoon air temperatures during heat events. Caution should be exercised when interpreting these results due to the limited number of heat event days in the data set

ΔTair = 5.76 - 0.09N1 - 2.66I1 - 3.29 C1 - 0.68D1 + 0.03Cup1 + e (Model Three)

Table 1.10: Regression Analysis for UHI Temperatures at 4 p.m. during Heat Events in Eight Jimeta Residential Neighborhoods during Two Clear Days in the dry season 2019

	Model 1			***Model 2***			***Model 3***		
Variable	B	SE	*Beta*	B	SE	*Beta*	B	SE	*Beta*
Neighborhood	-.13	.15	-.21	-.11	0.15	-.18	-.09	.16	-.15
% Impervious				-.68	5.11	-.05	-2.66	6.31	-.21
% Tree Canopy				-5.52	4.02	-.54	-3.29	12.02	-.32
Distance to Industry							-.68	.58	-.66

Upwind % Tree Canopy							.03	.15	.21
(Constant)	2.11*	.87		3.85	5.06		5.76	5.87	
n		16			16			16	
Adjusted R2			-.02			.11			.12
Change in R2						.24			.12

*p < .05. **p < .01. ***p < .005 (one-tailed tests).

Conclusion

Land covers, neighborhood building configurations, and adjacent heat sources and sinks are physical characteristics of neighborhoods that affect local air temperatures. This study examined the relative contribution of these physical characteristics to understand what factors researchers and planners should prioritize in neighborhood UHI analysis and UHI reduction programs. The main findings suggest the importance of 1) controlling for weather to isolate urban-induced warming, 2) the relative contribution of individual independent variables to UHI intensities, 3) the diurnal variation in UHI drivers, 4) variations in UHI drivers during heat events, and 5) the lack of association between UHI intensity and income in temperate moist climates. These findings are important for both UHI analysis and reduction efforts.

First, as past research has shown (Stewart, 2011; Bonacquisti *et al.*, 2006; Gedzelman *et al.*, 2003; Kim and Baik, 2002; Klysik and Fortuniak, 1999; McPherson *et al.*, 1997) controlling for weather (clear skies) appears to have isolated the effect of urban warming. This urban warming showed up in the larger ranges, we found of ΔTair between neighborhoods and in the O.L.S. regression analysis. Controlling for weather (clear skies) increased the range of UHI intensities (ΔTair) from 2.97ºC (62 days) to 4.15ºC (12 clear days). Controlling for clear skies also increased the explanatory power of the 2 a.m. UHI Model Three (adjusted R2 = 0.50 for 62 days and adjusted R2 = 0.68 for 12 clear days). During the day (4 p.m.) the change in the range of UHI intensities (ΔTair) was not as large as at night (from 2.28ºC for all 62 days to 2.85ºC for the 12 clear days). In addition, although the explanatory power of the 4 p.m. UHI Model Three improved controlling for clear skies (adjusted R2 = 0.17 for 62 days and adjusted R2 = 0.26 for 12 clear days). ΔTair was still more difficult to predict during the day than at night. For UHI analysis, researchers and planners should control for weather to isolate urban warming from other causes of warming (weather systems, maritime influences, topography, and distance between sites).

Second, Bivariate analysis identified the most significant relationships between the individual independent variables of land cover, neighborhood building configuration, and adjacent heat sources and sinks and ΔTair at 2 a.m. and 4 p.m. on the 12 clear days. The two independent variables with the highest correlation with ΔTair at 2 a.m. in the eight (8) residential neighborhoods were the percent impervious surface (.82) and percent tree canopy (-.72). The finding on impervious surface bivariate relationship with ΔTair is similar to the correlation Imoff and colleagues (2010) found between impervious surface and the difference in surface temperatures in the Chicago region (explained 89% of the variance in the difference in land surface temperature between urban and rural sites). The percent tree canopy bivariate relationship we found is nearly identical to what Hamada and Ohta (2010) found in Japan, where percent tree canopy in Nagoya explained 72% of the variance in ΔTair at 1 a.m. At 4 p.m. relationships were weaker than at 2 a.m. At 4 p.m. the independent variables with the highest correlation with ΔTair in the eight (8) residential neighborhoods were distance to upwind industrial sites (-.52) and adjacent upwind percent tree canopy (-.48). For UHI analysis, these finding provide further evidence of the warming effects of land cover variables on local air temperatures at night and how higher daytime wind speeds complicate late afternoon predictions (Imhoff *et al.*, 2010; Kuttler *et al.*, 1996; Yuan and Bauer, 2007; Dimoudi and Nikolopoulou, 2003; Zhang *et al.*, 2011).

Next, based on the bivariate analysis we choose two land cover variables (percent impervious surfaces and percent tree canopy) and two neighborhood building configuration (urban canyon ratio and orientation) to understand the relative importance of the combination of variables at night. For the afternoon, we choose two land cover variables (percent impervious surfaces and percent tree canopy) and two adjacent heat sources/sinks (upwind distance to industrial and percent tree canopy in the adjacent upwind area) to understand the relative importance of the combination of variables during the day. Through O.L.S. regression analysis we found that land cover variables were more important than neighborhood building configuration variables in predicting ΔTair on clear nights. On the 12 clear days, at 2 a.m. the percent impervious surface was the only significant predictor of ΔTair. At night, the contribution from impervious surfaces accounted for a +0.97ºC increase in air temperature for every 10% increase in amount of impervious surface. Yet, by 4 p.m. percent impervious surface was not a significant predictor of the ΔTair and distance to industry became significant. This finding is a bit higher than what Zhang and colleagues (2011) found at 17 sites in the Detroit area. They found that for every 10% increase in impervious surface area a site warmed by +0.40ºC at 5 a.m. and percent impervious was insignificant in the late afternoon (Zhang *et al*., 2011).

For UHI analysis, this suggests using percent impervious surfaces of a neighborhood to predict UHIs relative to building configuration. We found that building configuration was not a significant predictor of ΔTair in the eight neighborhoods. Building configuration is difficult to change and strategies to decrease impervious pavements and increase vegetation may prove more important in lessening UHI. This is consistent with other research that has shown the benefits of compact development in reducing the growth of UHIs. Compact development reduces the amount of natural land cover converted to impervious surface and reduces waste heat from the lower energy use that results from compact settlements (Stone *et al.*, 2007; Stone and Norman, 2006). Likewise to reduce UHIs, planners should look to reduce the amount of impervious surface to reduce nighttime air temperatures.

During the afternoon we found different drivers than at night. At 4 p.m., the contribution from upwind industrial sites accounted for a -.45ºC decrease in air temperature for every 1.0 km increase in distance from upwind industrial areas. Put another way, warming associated with industrial areas appears to be transported by higher afternoon winds to downwind neighborhoods. Neighborhoods further from industrial areas were cooler than neighborhoods with closer proximity to these areas. Yet, it is unclear from the analysis if the largest influence was from waste heat or large areas of impervious surface relative combined with a lack of vegetation that are common in industrial zones. For UHI analysis, it is much more difficult to predict afternoon UHI intensities than at night. In addition, researchers should include analysis of upwind factors. For UHI reduction, to reduce afternoon air temperatures, planners should target industrial sites for UHI reduction strategies and address waste heat, high amounts of impervious surface, and lack of vegetation. These findings suggest planners should provide incentives for retrofitting existing industrial sites and require new industrial sites install light or green roofs, permeable pavements, and shade trees to help reduce afternoon air temperatures downwind from industrial areas.

In terms of the variation in the physical drivers of UHI intensity between night and day, many of the differences are likely due to both differences in solar exposure and in wind speeds. At night, light winds and lack of incoming solar radiation likely strengthen localized effects of impervious surfaces. Yet, during the afternoon stronger winds and solar exposure make localized effects less important. During the day higher winds and high solar exposure complicate heating and cooling mechanisms. Higher winds during the afternoon mix the air near the surface. This reduces the influence of local physical characteristics and increases the area of influence. Increasing the effect upwind factors play in contributing to local warming. Researchers analyzing UHIs should avoid using daily averages to examine the physical drivers of UHI intensities, but analyze specific important times of day. Using averages may obscure influential patterns.

Fourth, during two clear heats event days land cover variables continued to be the only significant predictors. The 2 a.m. heat event analysis showed that Model Three explained more of the variance in air temperature difference (90%) than Model Three during the 12 UHI days (68%), while the 4 p.m. heat event analysis showed that Model Three explained less of the variance in air temperature difference (12%) than Model Three from the 12 UHI days (26%). At 2 a.m. both percent impervious surface and tree canopy were significant predictors of air temperature difference during heat events. On clear nights during heat events the percent impervious surface variable indicated a warming effect of +0.93ºC for every 10% increase in impervious surfaces. This increase in warmth is similar to the effect of impervious surface on the 12 clear days (+0.97ºC for every 10% increase). Yet, unlike the previous analysis for all 12 clear days during the two clear heat events tree canopy becomes a significant predictor of air temperature difference in the eight neighborhoods. Increasing the percentage of tree canopy by 10% in the eight residential neighborhoods of Jimeta resulted in a decrease in air temperature difference of -0.33ºC during heat events. Yet, no predictors were significant at 4 p.m. UHI analysis should collect weather data on heat event days due to public health implications. In addition, our findings suggest UHI reduction programs in mid-latitude temperate climates, such as Adamawa State Urban Planning Development Authority, should prioritize both reductions in impervious surfaces while adding vegetation to reduce nighttime temperatures during heat waves. More longitudinal research is needed on clear heat event days.

Finally, we found that lower income neighborhoods were not more likely to experience elevated air temperatures. This finding contradicts previous research showing a link between UHIs and neighborhood household income levels (Santamouris *et al.,* 2007; Harlan *et al.,* 2006, Solecki *et al.,* 2005; Jenerette *et al.,* 2007). In Jimeta's moist temperate climate vegetation does not align with income. The lowest income neighborhood, Doubeli ward, with an average household income in 2019 of N30,000 had more tree canopy (18.5%) and was cooler on average at both 2 a.m. and 4 p.m. than higher income neighborhoods Luggere ward NN33,000 with 4.7% tree canopy) and Nasarawo ward N41,000 with 13.2% tree canopy). Lower income neighborhoods were not associated with lower vegetation and higher air temperatures as in other cities that lie in drier climates where paying for irrigation was key to creating cooler microclimates. Other physical characteristics such as percent impervious surface and the distance to upwind industrial areas were more important in driving elevated air temperatures in the eight Jimeta residential neighborhoods. For UHI reduction, the biggest finding suggests that removing impervious surface is useful to lower nighttime air temperatures in temperate urban climates, especially on clear dry season nights. For instance if the City could reduce the amount of impervious surface in Luggerre ward by 5%, 10%, or 15% from its current 95.7%, the 2 a.m. UHI Model Three suggests that Luggerre ward is likely to reduce its UHI intensity. Based on predictions from the 2 a.m. Model Three for 12 clear days, Luggerre ward air temperature could be reduced from its current + 2.34ºC from Yola International Airport for 95.7% impervious surfaces to 1.77 ºC for 90% impervious, 1.28ºC for 85% impervious, and as low as 0.80ºC for 80% impervious. Methods to reduce impervious surface may include adding green roofs, installing permeable pavements on sidewalks, streets, and pathway, and removing any unnecessary impervious pavements. This illustrates the potential positive benefits from addressing the amount of impervious surfaces. The value of this study is that it provides a guide for researchers and planners to understand the relative contribution of using different physical characteristics to predict neighborhood UHIs. In addition, it provides guidance on potentially effective UHI reduction strategies.

Limitations:

This study has three important limitations. First, the number of neighborhoods included in the study was limited to eight. Although we were careful to include different neighbourhood physical characteristic types in the study, it does not allow us to make predictions for neighborhoods that substantially differ from the sites. In addition, the small number of sites and the fine scale of the study limit our ability to explain air temperatures between sites. Second, the River Benue breeze may complicate the analysis. Although we planned the study for March and April when the river breeze is diminished, from the data the River Benue is still a substantial influence even late into the dry season. We attempted to account for the River Benue's influence by including a variable for distance to River Benue. This variable was only significant at night and not during the afternoon when we might expect River cooling (Table 3.2). Finally, in the two month period we only were able to capture two major heat event days. This limits the confidence in the relationships between heat events and land covers' contribution to air temperature.

References

Akbari, H., Rose, L. S., and Taha, H. (2003). Analyzing the land cover of an urban environment using high-resolution orthophotos. *Landscape and Urban Planning, 63*, 1-14.

Baik, J., Kim, Y., and Chun, H. (2001). Dry and moist convection forced by an urban heat island. *Journal of Applied Meteorology, 40*, 1462-1475.

Bonacquisti, V., Casale, G. R., Palmieri, S., and Siani, A. M. (2006). A canopy layer model and its application to Rome. *Science of the Total Environment, 364*, 1-13.

Dimoudi, A., and Nikolopoulou, M. (2003). Vegetation in the urban environment: Microclimatic analysis and benefits. *Energy and Buildings, 35*, 69-76.

Djen, C. S., Jingchun, Z., and Lin, W. (1994). Solar radiation and surface temperature in Shanghai City and their relation to urban heat island intensity. *Atmospheric Environment, 28*(12), 2119-2127.

Gaffin, S. R., Rosenzweig, C., Khanbilvardi, R., Parshall, L., Mahani, S., Glickman, H., (2008). Variations in New York City's urban heat island strength over time and space. *Theory of Applied Climatology, 94*, 1-11.

Gartland, L. (2008). *Heat islands: Understanding and mitigating heat in urban areas*. Sterling, Virginia: Earthscan.

Gedzelman, S. D., Austin, S., Cermak, R., Stefano, N., Partridge, S. and Quesenberry, S., (2003). Mesoscale aspects of the urban heat island around New York City. *Theory of Applied Climatology, 75*, 29-42.

Gray, K. A., and Finster, M. E. (2000). *The urban heat island, photochemical smog, and Chicago: Local features of the problem and solution* Atmospheric Pollution Prevention Division U.S. Environmental Protection Agency.

Hamada, S., and Ohta, T. (2010). Seasonal variations in the cooling effect of urban green areas on surrounding urban areas. *Urban Forestry and Urban Greening, 9*, 15-24.

Harlan, S. L., Brazel, A. J., Prashad, L., Stefanov, W. L., and Larsen, L. (2006). Neighborhood microclimates and vulnerability to heat stress. *Social Science and Medicine., 63*, 2847-2863.

Imhoff, M. L., Zhang, P., Wolfe, R. E., and Bounoua, L. (2010). Remote sensing of the urban heat island effect across biomes in the continental USA. *Remote Sensing of Environment, 114*, 504 - 513.

Jenerette, D. G., Harlan, S. L., Brazel, A., Jones, N., Larsen, L., and Stefanov, W. L. (2007). Regional relationships between surface temperature, vegetation, and human settlement in a rapidly urbanizing ecosystem. *Landscape Ecology, 22*(3)

Kalkstein, L. S., and Davis, R. E. (1989). Weather and human mortality: An evaluation of demographic and interregional responses in the united states. *Annals of the Association of American Geographers, 79*, 44-64.

Kim, Y., and Baik, J. (2002). Maximum urban heat island intensity in Seoul. *Journal of Applied Meteorology, 41*, 651- 659.

Klysik, K., and Fortuniak, K. (1999). Temporal and spatial characteristics of the urban heat island of Lodz, Poland. *Atmospheric Environment, 33*, 38885-3895.

Kuttler, W., Barlag, A., & Robmann, F. (1996). Study of the thermal structure of a town in a narrow valley. *Atmospheric Environment, 30*(3), 365-378.

McPherson, G. E., Nowak, D., Heisler, G., Grimmond, S., Souch, C. and Grant, R., (1997). Quantifying urban forest structure, function, and value: The Chicago urban forest climate project. *Urban Ecosystems,* (1), 49-61.

Memon, R. A., Leung, D. Y. C., and Chunho, L. (2007). A review on the generation, determination, and mitigation of urban heat island. *Journal of Environmental Sciences, 20*, 120-128.

O'Neill, M. S., Zanobetti, A., and Schwartz, J. (2005). Disparities by race in heat-related mortality in four U.S. cities: The role of air conditioning prevalence. *Journal of Urban Health, 82*(2)

Oke, T. R. (1988). Street design and urban canopy layer climate. *Energy and Buildings, 11*, 103-113.

Oke, T. R. (2004). *Initial guidance to obtain representative meteorological observations at urban sites* No. 81) World Meteorological Organization.

Santamouris, M., Kapsis, K., Korres, D., Livada, I., Pavlou, C., and Assimakopoulos, M. N. (2007). On the relation between the energy and social characteristics of the residential sector. *Energy and Buildings, 39*, 893-905.

Solecki, W., Rosenzweig, C., Parshall, L., Pope, G., Clark, M., Cox, J., (2005). Mitigation of the heat island effect in urban New Jersey. *Environmental Hazards, 6*, 39-49.

Stewart, I. D. (2011). A systematic review and scientific critique of methodology in modern urban heat island literature. *International Journal of Climatology, 31*, 200-217.

Stone, B., and Norman, J. M. (2006). Land use planning and surface heat island formation: A parcel-based radiation flux approach. *Atmospheric Environment, 40*, 3561-3573.

Stone, B., Jr. (2005). Urban heat and Air Pollution: An emerging role for planners in the climate change debate. *Journal of the American Planning Association, 71*(1), 13-25.

Stone, B., Jr. (2012). *The city and the coming climate: Climate change in the places we live*. New York, NY: Cambridge University Press.

Stone, B., Jr., Mednick, A. C., Holloway, T., and Spak, S. N. (2007). Is compact growth good for air quality? *Journal of the American Planning Association, 73*(4), 404-418.

Svensson, M. K. (2004). Sky View Factor Analysis – implications for urban air temperature differences. *Meteorological Applications, 11*, 201-211.

Wilby, R. L. (2003). Past and projected trends in London's urban heat island. *Weather, 58*, 251-260.

Yuan, F., and Bauer, M. E. (2007). Comparison of impervious surface area and normalized difference vegetation index as indicators of surface urban heat island effects in Landsat imagery. *Remote Sensing of Environment*, (106), 375-386.

Zhang, K., Oswald, E., M., Brown, D. G., Brines, S. J., Gronlund, C. J., White-Newsome, J. L., (2011). Geostatistical exploration of spatial variation of summertime temperatures in the Detroit metropolitan region. *Environmental Research, 111*, 1046-1053.